# Some Aspects of $\pi N$ Scattering in the $P_{11}$ State*

HYMAN GOLDBERG
*Laboratory of Nuclear Studies, Cornell University, Ithaca, New York*
(Received 11 October 1966)

A study of $\pi N$ scattering in the $P_{11}$ state is presented within the framework of the unitary $f$ matrix, or boundary-condition model. Inelastic channels treated are $\sigma N$ and $\pi N^*$, where $\sigma$ is a $I=0$, $J=0^+$ $\pi\pi$ pair. The mass spread of the inelastic channel is taken into account in a unitary manner. It is apparent from an examination of the fits to the data that the $\sigma N$ channel is vastly preferred as an inelastic mode; the reasons are fully discussed in the text. The crossover of the phase shift at 175 MeV is seen to be impossible with a conventional force input. From a study of eigenphases we conclude that there is no Breit-Wigner resonance in any eigenchannel. Also, by means of the eigenphase representation, we demonstrate a source of possible discrepancies in recent phase-shift analyses. The value of $m_\sigma$ obtained for a best fit, 550 MeV, is compared with other values obtained by various authors. Finally, we examine the effects of the $P_{11}$ "object" on the Gell-Mann–Okubo mass formula.

## I. INTRODUCTION

THERE now exists a significant body of data to support the conclusion that "something" is occurring in the $\pi N$, $I=\frac{1}{2}$ scattering state in the 1400–1500 MeV barycentric energy region. This may be summarized as follows:

(*i*) *Direct $\pi p$ scattering.* Bareyre *et al.*,[1] in plotting the $\pi N$, $I=\frac{1}{2}$ elastic cross section, have found a shoulder in the curve at about 200 MeV (lab K. E.) below the well-known $N^*(1512)$. They then obtain a good fit to the curve in the whole region by the use of two Breit-Wigner resonances: one with $J=\frac{1}{2}$, the other with $J=\frac{3}{2}$, and a small (~5 mb), slowly increasing background term. The parameters of the resonance curves they obtained may be listed as follows.

| | "Shoulder" | "Second" resonance |
|---|---|---|
| c.m. energy | 1400 MeV | 1510 MeV |
| Pion lab kinetic energy, $T_\pi$ | 430 MeV | 600 MeV |
| Total width, $\Gamma$ | 240 MeV | 140 MeV |
| Elasticity, $\Gamma_{el}/\Gamma$ | 0.65 | 0.75 |
| Elastic cross section at peak | 15 mb | 26 mb |
| $J$ | $\frac{1}{2}$ | $\frac{3}{2}$ |

(*ii*) *Peaks in $N^*$ production cross sections.* Studies of[2] $\bar{K}p \to \bar{K}N^*$ and $pp \to NN^*$ (Refs. 3 and 4) have indicated enhancement at $N^*$ masses near 1400 MeV. The Brookhaven data[4] are particularly striking in that the 1400 peak dominates the inelastic spectrum at low $t$ and high $s$. The width quoted is 180±50 MeV, reasonably consistent with the assignment of Bareyre *et al.*

(*iii*) *Phase-shift analyses.* A number[5–8] of recent phase-shift analyses of $\pi p$-scattering data concur about an enhancement in the $P_{11}$ amplitude in the presently discussed energy region. Some of these differ quite markedly in the actual behavior of the real part of the phase shift (hereafter called "the phase shift") but, as emphasized by Dalitz and Moorhouse[9] and by the author,[10] most of these are consistent with strong (but nonresonant) scattering in some underlying eigenphase. The enhancement is strong enough, though, to produce a bump in cross sections plotted from the phase shifts. In common to most of these analyses is a large inelasticity ($\eta=0.1$ to 0.3). The cross sections plotted from these analyses are also more or less in agreement with the cross section fits of Bareyre *et al.*[1] [see paragraph (*i*) above]. The comparison is shown in Fig. 3 of Ref. 9.

(*iv*) *Photoproduction of $\pi^0$.* There are two pieces of evidence from $\pi^0$ photoproduction data.[11] (1) a large value of $A_1$ in the cross-section expansion $k^2 d\sigma/d\Omega = \sum_n \cos^n\theta$ in the vicinity of the second resonance. This indicates a strong interference in this region between two states of opposite parity. One of these is presumably the $\frac{3}{2}^-$ (1512-MeV) resonance. The proposed other one is, of course, our $\frac{1}{2}^+$ object; (2) sizeable recoil proton polarization at 90°, again near the second resonance. This would not occur if a single parity were contributing to the scattering, and again indicates an interference of the type just described. The positive-parity object could be the 33 resonance, but because of the large energy differences, the $P_{11}$ object is a much more plausible candidate.

In view of these data, some attempt at determining a plausible model for the scattering seems warranted. In a recent $N/D$ calculation, Coulter and Shaw[12] find that the usual elastic forces ($N_{33}^*$ exchange, $\rho$ exchange, $N$ exchange, etc.,) can lift the $P_{11}$ phase shift to perhaps 40° at 600 MeV (pion lab kinetic energy), but are quite

* Supported in part by the U. S. Office of Naval Research.
[1] P. Bareyre, C. Bricman, G. Valladas, G. Villet, J. Bizard, and J. Seguinot, Phys. Letters **8**, 137 (1964).
[2] S. L. Adelman, Phys. Rev. Letters **13**, 555 (1964).
[3] G. Cocconi *et al.*, Phys. Letters **8**, 134 (1964).
[4] E. W. Anderson *et al.*, Phys. Rev. Letters **16**, 855 (1966).
[5] L. D. Roper, Phys. Rev. Letters **12**, 340 (1964).
[6] B. H. Bransden, P. J. O'Donnell, and R. G. Moorhouse, Phys. Letters **11**, 339 (1964).
[7] P. Auvil, A. Donnachie, A. T. Lea, and C. Lovelace, Phys. Letters **12**, 76 (1965).
[8] P. Bareyre, C. Brickman, A. V. Stirling, and G. Villet, Phys. Letters **18**, 342 (1965).
[9] R. H. Dalitz and R. G. Moorhouse, Phys. Letters **14**, 159 (1965).
[10] H. Goldberg, Phys. Rev. **151**, 1186 (1966).
[11] See, for instance, G. Källén, *Elementary Particle Physics* (Addison-Wesley Publishing Company, Inc., Reading, Massachusetts), pp. 160, 165.
[12] P. W. Coulter and G. L. Shaw, Phys. Rev. **141**, 1419 (1966).

insufficient to produce a resonance. However, these authors find that an experimental inelasticity parameter inserted into the Frye-Warnock[13] modification of the $N/D$ equations will boost the elastic phase shift to 70° at 500 MeV before it drops off. It will be the purpose of this paper to test several possibilities for the inelastic channel within the framework of a simple unitary model. The results may be stated as follows: (1) Coupling to a $p$-wave $N_{33}^*$ channel can provide for a rise in the phase shift, but the $p$-wave nature of the final state does not allow the rapid drop in the phase shift after 600 MeV which is indicated in several analyses. In addition, the requirement of a rapid onset of absorption, as indicated by the data, forces the coupling to be very high (again because of the $p$ wave), and this in turn requires the elastic $\pi N$ attraction to stay very small in order to fit the lower-energy phase shifts. Qualitative (i.e., Born) considerations of the forces involved support a rather *large* elastic attraction. (2) Coupling to a continuum distribution of $N\sigma$ $s$-wave channels can satisfactorily explain most of the interesting aspects of the data. By "$\sigma$" we mean nothing more than an $I=0$, $J^P=0^+$ pair of pions. We find that the best fit has the $\sigma$ mass distribution centered at 550-MeV $\pi\pi$ c.m. energy, with an effective width of 100 MeV. With this channel it is found that a moderately strong diagonal $\pi N$ force is required, combined with relatively weak coupling. The results are insensitive to the average $\sigma N$ force, as long as it is attractive.

The plan of the paper is as follows: Sec. II presents some qualitative discussion on the pros and cons for the various inelastic channels considered. Section III discusses the unitary model used and its modifications for the applications which are the subject of the paper. Section IV is a brief detailing of the data chosen to be fitted. Section V consists of a detailed discussion of the parameters giving best fits to the selected data, and of the information they convey about the forces involved. In Sec. VI we discuss the eigenscattering of the system in a particle approximation to the $\pi\pi$ pair. Section VII deals with possible roles of the $P_{11}$ bump in $SU_3$ dynamics, and Sec. VIII presents a summary and conclusions.

## II. HEURISTIC DISCUSSION OF POSSIBLE INELASTIC CHANNELS

It is by now well established[14] that in the region of interest there is present a great deal of $N^*(1238)$ production. But it has also become apparent[15] that the $\pi^+\pi^-$ effective-mass distributions at these energies show peaking towards the high-energy end which cannot be explained by recent modifications[16] of the Lindenbaum-Sternheimer isobar model. This anomaly does not occur in the $\pi^\pm\pi^0$ mass distributions, which has led to speculations that there is an important contribution from a strong $I=0$ interaction in the $\pi\pi$ final state. If we assume that this state also has $J^P=0^+$, we are led to consider this as an important inelastic channel. As stated above, we shall for brevity refer to the $I=0$, $J=0^+$ state as a "$\sigma$" pair of pions. We now present some qualitative arguments in favor of the $N\sigma$ channel over the $\pi N^*$ channel as responsible for the $P_{11}$ enhancement.

(1) First, consider isotopics. If we assume that the $N^*$ is produced via the $N$-exchange process shown in Fig. 1, standard recoupling procedures[17] show that the $I=\frac{1}{2}$ channel is favored over the $I=\frac{3}{2}$ channel only by a factor of 8/5 in the *square* of the amplitude. On the other hand, production of an $I=0$ pair of pions is *only* possible in the total $I=\frac{1}{2}$ state. The clue now lies in the phase-shift analyses, where we find, in most cases, that $P_{31}$ has very little absorption compared to $P_{11}$. This strongly refutes the $N^*$ production and supports the $\sigma$-production hypothesis.

(2) Secondly, there is an angular-momentum argument. From $J^P$ considerations, the $\sigma$ pair would be produced in an $S$ state with respect to the final nucleon, the $N^*$ in a $P$ state with respect to the final pion. This would inhibit production of the $N^*$ near its threshold (say around 300-MeV pion lab K.E.). All the phase-shift analyses show $\eta$, the inelastic parameter for the $P_{11}$ partial wave, falling fairly rapidly near 300 MeV. So unless there is rather spectacular coupling, this behavior would again seem to support the $\sigma N$-type inelasticity.

(3) Finally, we present a somewhat intuitive discussion of energetics. Suppose that we imagine that the target nucleon consists of a nucleon core surrounded by a pion cloud. The cloud pion is confined to a volume which dictates a mean pion 3-momentum of about 1 (in units of $m_\pi c$) because of the uncertainty principle. Thus we set $\Delta p\sim 1$. Assume also (without any deep justification) that we may neglect mass-shell corrections, and give the cloud pion an average total energy of $(1^2+1^2)^{1/2}=\sqrt{2}$ during the collision time. This we call $\Delta E$. Then for a collision with an incoming pion of momentum $p$ and energy $E=(p^2+1)^{1/2}$, the square of

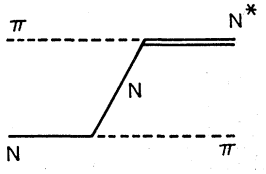


FIG. 1. Diagram describing proposed dominant $N^*$ production process.

[13] G. Frye and R. Warnock, Phys. Rev. **130**, 478 (1963).
[14] R. A. Burnstein, G. R. Charleton, T. B. Day, G. Quareni, A. Quareni-Vignudelli, G. B. Yodh, and I. Nadelhaft, Phys. Rev. **137**, B1044 (1965); C. N. Vittitoe, B. R. Riley, W. J. Fickinger, V. P. Kenney, J. G. Mowat, and W. D. Shephard, *ibid.* **135**, B232 (1964).
[15] J. Kirz, J. Schwartz, and R. Tripp, Phys. Rev. **130**, 2481 (1963).
[16] M. G. Olsson and G. B. Yodh, Phys. Rev. **145**, 1309 (1966).
[17] P. A. Carruthers and J. P. Krisch, Ann. Phys. (N. Y.) **33**, 1 (1965).

the total energy in the $\pi\pi$ c.m. is given by

$$m^2=(E+\Delta E)^2-(\mathbf{p}+\Delta\mathbf{p})^2$$
$$=2+2E\Delta E-2\mathbf{p}\cdot\Delta\mathbf{p}.$$

The average value of the last term is zero, and its rms derivation from 0 is $2p\ \Delta p$. For an incoming pion with kinetic energy 450 MeV, (c.m.: 1410 MeV) $E=0.59$ GeV$=4.2\,\mu$, $p=4.1\,\mu$. Then the above equation becomes

$$m^2=13.8\pm5.7\,\mu^2,$$

or

$$m=520\pm107\text{ MeV}.$$

At this point, the argument runs as follows: If the $\pi\pi$ interaction in the $I=0$ state is strong in this energy region, then we expect that this cloud interaction will greatly enhance $I=\frac{1}{2}$ $\pi N$ scattering in the region just below the 1512 resonance.[18,19]

The threshold for *producing* a pair of pions with an effective mass of 520 MeV is at an energy of 1440 MeV in the $\pi N$ c.m. system. This is also in the region of interest. Thus, if the $\pi\pi$ interaction is significant in the $\sigma$ state near 500 MeV in the $\pi\pi$ c.m. system we not only would get an enhancement of $P_{11}$ scattering, but we would also produce these $\sigma$ pairs in an $S$ state with respect to the nucleon, leading to a Ball-Frazer[20] type of enhancement. Hence there is some expectation of success with this mechanism. In fact, we shall find that producing $\sigma$'s having a mean mass of 550 MeV and a spread of 100 MeV will do the trick.

No such support can be given to $N^*(1238)$ production. At 450 MeV in the lab we are 70 MeV beyond threshold for producing $N^*$ at its peak. Since the production can occur only in the $p$ state relative to the final pion, by the time we have escaped the region of depression due to the angular-momentum barrier, we are quite far from the $N^*$ threshold region. This can be overcome by the presence of extremely high coupling which is inexplicable by standard Feynman-graph intuition. We shall in fact find some such fit, but it is quite unsatisfactory on several additional counts. We now turn to examine the model with which we test these hypotheses.

## III. THE UNITARY DYNAMICAL MODEL

### A. General Considerations

Of necessity in any inelastic calculation are (1) unitary coupling of channels, (2) correct threshold dependences, and other kinematic effects, and (3) reasonable physical interpretation of parameters involved. The coupled $N/D$ equations have been used in the past to fulfill these criteria. However, two channel problems have usually been treated in pole approximations to the unphysical singularities. What is worse, there has been no kinematically realistic attempt within this framework at including the width of the particle produced.[21]

We shall settle here for a simpler model which incorporates all the above desirable features, and allows for simple inclusion of "woolly cusps."[22] This is the coupled-channel boundary-condition model (BCM), which has been used previously[23] for an exploration of the $D_{13}$ resonance.

More elaborate discussion of the theory underlying the model and its applicability to strong-interaction dynamics has been developed elsewhere.[23–25] Suffice it to say that the model is based on the following assumptions.

(1) Relativistic, *free*, configuration-space wave functions outside some interaction radius are a plausible concept. The value (of the radius) should make a valid connection with the range of the expected forces. Relativity is introduced through the kinematical definition of the momentum.

(2) In the energy region where the model is applied, the diagonal forces in any one channel would not alone create a resonant situation. The way in which this statement is expressed in the model is through the constancy of the Wigner-Eisenbud $R$ matrix[26] over the energy region of interest. Equivalently, it means the constancy of all logarithmic derivatives of the wave functions at the radius of interest. We shall deal with the inverse of the $R$ matrix, and call it the $f$ matrix.

The plan of the rest of Sec. III is as follows: First we present derivations of the effective logarithmic derivative of the elastic-channel wave function at the radius $r_0$. This will be done for the 2-channel and many-channel "woolly cusp" cases. Then we give the relation between this quantity (to be denoted by $f_{\text{eff}}$) and the elastic $S$-matrix element $\eta e^{2i\delta}$.

### B. 2-Channel Case

Suppose we have 2-channel scattering, described by free radial wave functions $u_1/r$ and $u_2/r$ outside an

[18] It is possibly significant that if one raises the kinetic energy of the incoming pion to 600 MeV, then the previous equation becomes $m=580\pm125$ MeV. In this region one might begin to feel the enhancement due to strong $I=1$, $J=1$ (tail of the $p$ meson) $\pi\pi$ scattering in the cloud, although the production threshold in the lab is at 870 MeV. This may be some justification for the virtual production mechanism used by some authors to explain the $D_{13}$ resonance (Refs. 19, 23).

[19] P. Carruthers, Ann. Phys. (N. Y.) **14**, 229 (1961); L. F. Cook, Jr., and B. W. Lee, Phys. Rev. **127**, 297 (1962); J. S. Ball, W. R. Frazer, and M. Nauenberg, *ibid.* **128**, 478 (1962).

[20] J. S. Ball and W. R. Frazer, Phys. Rev. Letters **7**, 204 (1962).

[21] See, however, J. S. Ball and P. Thurnauer [Phys. Rev. **136** B529 (1964)], for a discussion of the analyticity properties of a simplified $N/D$ production model including a resonant-mass spectrum for the produced particle.

[22] M. Nauenberg and A. Pais, Phys. Rev. **126**, 360 (1961).

[23] H. Goldberg and E. L. Lomon, Phys. Rev. **134**, B659 (1964). The prescription presented in this reference for including the width of the produced particle is incomplete. A better prescription is presented in the present paper.

[24] H. Feshbach and E. L. Lomon, Ann. Phys. (N. Y.) **29**, 19 (1964).

[25] H. Goldberg and E. L. Lomon, Phys. Rev. **131**, 1290 (1963).

[26] E. P. Wigner and L. Eisenbud, Phys. Rev. **72**, 29 (1947).

interaction radius $r_0$. The boundary-condition-model equations are

$$r_0\begin{bmatrix} du_1/dr \\ du_2/dr \end{bmatrix}_{r=r} = \begin{bmatrix} f_1 & f_c \\ f_c & f_2 \end{bmatrix}\begin{bmatrix} u_1 \\ u_2 \end{bmatrix}_{r=r_0}, \quad (1)$$

with the condition that $r_0$ correspond meaningfully with the distance at which the short-range forces become important; also, corresponding to (2) above, all the $f$'s are constant. The $f$ matrix is Hermitian and symmetric as a consequence of unitarity and time-reversal invariance.[26]

If channel 2 is a channel which opens at some threshold, then $u_2$ has the form

$$u_2(k_2r)=A_2rh_{l_2}(k_2r), \quad (2)$$

where $A_2$ does not depend on $r$ and is proportional to the $S$-matrix element $S_{12}$; $k_2$ is the c.m. momentum in channel 2; $l_2$ is the orbital angular momentum quantum number in channel 2; $h_l(z)$ is the outgoing spherical Hankel function of order $l$.[27]

From the properties of the Hankel function, we can write

$$r_0(du_2/dr)_{r=r_0}=\theta_2(k_2r_0)u_2(r_0), \quad (3)$$

where $\theta_2$ is some polynomial in $k_2r_0$ and $(k_2r_0)^{-1}$. Substituting (3) into (1), we obtain

$$r_0\left(\frac{du_1}{dr}\right)_{r=r_0}=\left[f_1+\frac{f_c^2}{\theta_2(k_2r_0)-f_2}\right]u_1(r_0)\equiv f_{\text{eff}}u_1(r_0). \quad (4)$$

At the end of the section we give the derivation of $\eta$ and $\delta$ from $f_{\text{eff}}$.

Consider first the interesting case of $S$-wave production, i.e., $l_2=0$. Then from (2) and (3),

$$\theta_2=ik_2r_0. \quad (5)$$

In a region not too far below threshold we shall make the analytic continuation

$$k_2\rightarrow ik_2. \quad (6)$$

Both above and below threshold we define $k_2$ through

$$k_2^2=(W^2-(M+m)^2)(W^2-(M-m)^2)/4W^2, \quad (7)$$

where $W$ = total energy in the c.m. system; $m$ = mass of particle produced, and $M$ = mass of nucleon. Then from (4), (5), and (6) we have that

(*i*) Below threshold ($W<M+m$)

$$\text{Re}f_{\text{eff}}=f_1-f_c^2/(|k_2|r_0+f_2), \quad (8)$$

$$\text{Im}f_{\text{eff}}=0. \quad (9)$$

(*ii*) Above threshold[28]

$$\text{Re}f_{\text{eff}}=f_1-f_c^2f_2/((k_2r_0)^2+f_2^2), \quad (10)$$

$$\text{Im}f_{\text{eff}}=-f_c^2(k_2r_0)/((k_2r_0)^2+f_2^2). \quad (11)$$

It is a consequence of the Wigner form of causality that in the elastic-scattering region $df_{\text{eff}}/dW\leq 0$.[24] This is seen to be satisfied by the expression (11) above. It is also known that a Breit-Wigner resonance will result from $f_{\text{eff}}$ decreasing *linearly* through 0 at the resonance energy.[20] Differentiating (8), we obtain, for $k_2$ near zero

$$\frac{df_{\text{eff}}}{dW}=-\frac{f_c^2}{f_2^2}r_0(M+m-W)^{-1/2}\left(\frac{2Mm}{M+m}\right)^{1/2}. \quad (12)$$

This is a much faster rate than that required for a resonance, and will cause a steep rise in the phase shift just below threshold. Of course, this extreme behavior does not continue past threshold where the onset of inelasticity depletes the elastic channel of its fast rise. From (10), it is easy to see that $d(\text{Re}f_{\text{eff}})/dW=\text{const}>0$ after threshold, thus violating Wigner's condition. This does not matter since we are in an inelastic region. But the upshot of this discussion is that we may expect a large decrease in $f_{\text{eff}}$ below threshold, leading to a considerable rise in the elastic phase shift. If we are (*i*) quite near threshold, and (*ii*) the production is $S$ wave, and (*iii*) $f_2$ *is not too large*, then we can expect the Ball-Frazer effect *with only moderate coupling* $f_c^2$. It is to be noted that we are slightly displaced from the Ball-Frazer region in that the major rise in the phase shift in the present analysis occurs *just below* threshold rather than *just after* threshold. In practice, this is a negligible difference because the threshold is usually "woolly."[22] By this we shall mean that the three-particle aspect of the final state makes itself felt in some way.

### C. Generalization to "Woolly Cusps"

We go back to the basic equation (1), and look for the effects of producing 3-particle states. The position is taken, that if in some manner two of the particles are strongly correlated over the energy region in question, we may consider the three-particle channel as consisting of many two-particle channels with the correlated pair in question having a continuous distribution of masses. In this we shall follow quite closely the assumptions made by Nauenberg and Pais.[22]

Suppose for a moment that the variable mass of the pair produced forms a closely spaced discrete set. Then

[27] L. I. Schiff, *Quantum Mechanics* (McGraw-Hill Book Company, Inc., New York, 1955), p. 79.

[28] In the Appendix of a previous paper (Ref. 25) the negativeness of $\text{Im}f_{\text{eff}}$ is seen to be a consequence of unitarity.

[29] J. M. Blatt and V. F. Weisskopf, *Theoretical Nuclear Physics* (John Wiley & Sons, Inc., New York, 1952), p. 400.

we rewrite Eq. (1) in the form

$$r_0\left[\frac{du(r)}{dr}\right]_{r=r_0}=f_1u(r_0)+\sum_m f_c(m)v(m,r_0),$$

$$r_0\left[\frac{dv(m,r)}{dr}\right]_{r=r_0}=f_c(m)u(r_0)+\sum_{m'} f_2(m,m')v(m',r_0). \quad (13)$$

Note that $u(r)$ does not depend on the variable $m$, and that the $f$'s are still energy-independent, although strongly $m$-dependent.

Now set

$$f_c(m)=f_c\phi(m), \quad (14)$$

where $f_c$ is a constant, and $\phi(m)$ is a real, normalized weighting function related to the mass distribution of the pair of particles correlated in the final state. The factorization (14) is done without loss in generality.

However, we now make the assumption that $f_2(m,m')$ may be factored as

$$f_2(m,m')=f_2\phi(m)\phi(m'). \quad (15)$$

This is a statement of the independence of mass distributions in the scattering

$$\text{channel } 2(m)\longrightarrow \text{channel } 2(m').$$

As before, the outgoing nature of the $v$ channels allows us to write

$$r_0[dv(m,r)/dr]_{r=r_0}=\theta(m)v(m,r_0), \quad (16)$$

suppressing the energy and $l$ dependence of $\theta$. Substituting (14), (15), and (16) into (13), we solve for $v(m,r)$;

$$v(m,r_0)=\frac{f_c\phi(m)u(r_0)}{\theta(m)}+\frac{f_2\phi(m)C(r_0)}{\theta(m)}, \quad (17)$$

with $C(r_0)=\sum_m \phi(m)v(m,r_0)$. It is assumed that we are not at a point where $\theta=0$. Multiplying (17) by $\phi(m)$ and summing, we obtain an equation for $C(r_0)$;

$$C(r_0)=\left[\sum_m\left(\frac{\phi^2(m)}{\theta(m)}\right)\right][(f_cu(r_0)+f_2C(r_0))], \quad (18)$$

whence

$$C(r_0)=f_cu\Big/\left\{\left[\sum_m\left(\frac{\phi^2(m)}{\theta(m)}\right)\right]^{-1}-f_2\right\}. \quad (19)$$

After substitution into Eq. (13) and conversion to an integration, we emerge with

$$r_0(du/dr)_{r=r_0}=f_{\text{eff}}u(r_0), \quad (20)$$

where

$$f_{\text{eff}}=f_1+f_c^2\Big/\left\{\left[\int\frac{\phi^2(m)dm}{\theta(m)}\right]^{-1}-f_2\right\}. \quad (21)$$

The lower limit on the integration is $2\mu$ if we correlate the two pions, or $M+\mu$ if we correlate the nucleon and one of the pions.

So far $\phi(m)$ is arbitrary, and for any specific choice the integral in (21) may be done numerically. There is, however, one choice of the mass distribution which makes it possible to evaluate the integral in (21) analytically to a good approximation; that is, if $\phi^2(m)$ is of the Breit-Wigner form

$$\phi^2(m)=\frac{\Gamma/2\pi}{(m-m^*)^2+\frac{1}{4}\Gamma^2}.$$

This choice of $\phi$ implies an enhancement of effective masses in the region of $m=m^*$, with a spread $\Delta m\sim\Gamma$. Making this choice and extending the lower limit of integration in Eq. (21) to $-\infty$, we find, by contour integration, that

$$f_{\text{eff}}=f_1+\frac{f_c^2}{\theta(m^*-\frac{1}{2}i\Gamma, W)-f_2}. \quad (22)$$

The effect of extending the domain of integration over $m$ from its actual lower limit to $-\infty$ is small. The required criterion is that $\frac{1}{2}\Gamma$ be a few times less than $m^*-2\mu$ or $m^*-(M+\mu)$, depending on whether we are correlating the $\pi\pi$ pair, or the $N\pi$ pair. In the cases considered in this paper, the error entailed is estimated as 10–15%.

Equation (22) is seen to adhere to the usual prescription of giving the mass a negative imaginary part. It can also be shown that this approximation retains unitarity, in that $\text{Im}f_{\text{eff}}$ remains $<0$.

We now explore the function $\theta$ for the two cases under consideration.

*Case 1: S-Wave Production of a Pair of Pions*

In this case, we have, from the definition (3) of $\theta$, that

$$\theta(m,W)=iK(m,W), \quad (23)$$

where

$$K(m,W)=\left[\frac{[W^2-(M+m)^2][W^2-(M-m)^2]}{4W^2}\right]^{1/2}. \quad (24)$$

$\theta(m^*-\frac{1}{2}i\Gamma,W)$ is obtained by making the indicated substitution for $m$.

*Case 2: P-Wave Production of N* Pion Final State*

Here, from the definition of $\theta$, [Eq. (3)] and the definition of the $l=1$ Hankel function

$$\theta(m,W)=i(x-1/(x+i)),$$
$$x=K(m,W)r_0. \quad (25)$$

In this case

$$K(m,W)=\left[\frac{[W^2-(m+\mu)^2][W^2-(m-\mu)^2]}{4W^2}\right]^{1/2}. \quad (26)$$

Again, $\theta(m^*-\frac{1}{2}i\Gamma, W)$ is obtained by making the indicated substitution for $m$.

### D. Derivation of S-Matrix from an Effective Logarithmic Derivative

Here we repeat for convenience the derivation given in Ref. 23. The reduced radial wave function in the elastic channel is given by

$$u(kr)=\phi^*(kr)+S(k)\phi(kr), \tag{27}$$

where the channel subscripts on $S=\eta e^{2i\delta}$ and the orbital-angular momentum subscript $l$ on $\phi$ will be henceforth understood. The asterisk denotes complex conjugation.

$\phi$ is the outgoing irregular solution of the free-reduced radial Schrödinger equation with c.m. momentum $k$. We normalize $\phi$ so that

$$\phi(z)=zh_l^{(1)}(z), \tag{28}$$

where $h_l^{(1)}(z)$ is the outgoing spherical Hankel function of order $l$.[27]

From the general relationship [Eq. (20) or (4)]

$$r_0(du/dr)_{r=r_0}=f_{\rm eff}(W)u(kr_0)$$

and Eq. (27) we obtain the relation between $S$ and $f_{\rm eff}$

$$S=-\left(\frac{f_{\rm eff}\phi^*-x\phi^{*\prime}}{f_{\rm eff}\phi-x\phi'}\right). \tag{29}$$

Thus, below threshold where $f_{\rm eff}$ is real [e.g., Eq. (9)], $|S|=1$, as required by unitarity. Also, given $f_{\rm eff}$, it is a trivial matter to obtain the elastic phase shift and the inelastic parameter $\eta$ from Eq. (29).

### E. Résumé

We have set up the equations which will yield a unitary $S$ matrix for the multichannel problem, where the inelastic channel has a Breit-Wigner mass distribution for one pair of particles. The final states to be considered are (1) $N_{33}^*+\pi$ (2) $N+\sigma$, where $\sigma$ is the state of two pions with $I=0$, $J^P=0^+$. The channel quantum numbers otherwise are, of course, $J^P=\frac{1}{2}^+$, $I=\frac{1}{2}$.

In the case of an $N_{33}^*$ inelastic channel, the model has 4 unknown parameters: $r_0$, $f_1$, $f_2$, and $f_c^2$. We expect $r_0$ to correlate well with the range of forces involved in the problem ($\frac{1}{4}$ to $\frac{1}{2}\mu^{-1}$). Here $f_1$ will indicate the strength of the diagonal $\pi N$ force in the $P_{11}$ channel, which is expected to be quite attractive in the 300–700 MeV region[30]; $f_2$ will give us the diagonal $\pi N^*$ force in this channel, and $f_c^2$ is a measure of the coupling strength between channels. The connection between the $f$'s and the forces will be made later.

In the case of $\sigma$ production, there are, in addition to the parameters just discussed, a mass parameter giving the center of the $\sigma$ mass distribution, and a width parameter describing the breadth of the distribution. (These parameters are taken as "known" in the case of $N^*$ production.) We now proceed to show the best fits to a subset of the data.

## IV. DATA TO BE FITTED

Because there are many pieces of data, we must be somewhat discriminatory in making a choice in the sample to be fitted. The choice has been the preferred solution in the phase-shift analysis of Auvil *et al.*[7] We have done this for essentially two reasons: (1) This solution gives a reasonably good fit to all existing data as well as to the Breit-Wigner curve proposed by Bareyre *et al.*[1] (see Sec. I) to account for the shoulder in the $I=\frac{1}{2}$ elastic cross section. (2) It does not employ an energy dependent[5,6] analysis in the highly absorptive region. The phase shift may change quite rapidly in such a region,[9,10,20] and it is difficult to estimate how well the energy dependences used by various authors can reproduce this variation. The $\eta$ and $\delta$ from this analysis may be seen on all the figures where the theoretical curves are plotted.

## V. FITS TO THE DATA

Before discussing the interesting fits to the data, along with the model parameters associated with them, we make the following comment about the range parameter $r_0$:

All fits required a radius $r_0$ in the near vicinity of $0.30\mu^{-1}$. This is in good agreement with our pre-existing prejudices about the range of the strongest forces contributing. For instance, it is well known[30,31] that the $N_{33}^*$ exchange force is very strong in the $P_{11}$ partial wave. Using an argument given by Singh,[32] the range of this force in this energy region is found to be about $0.13\mu^{-1}$. The range of $\rho$ exchange is about $0.19\mu^{-1}$. However, these are balanced by the probable longer-range nature of the production process ($1\mu^{-1}$ in the case of $\sigma$ production, if the process goes by one pion exchange) and of the final-state interaction. In any case, it is a perfectly reasonable range.

We now turn to a detailed discussion of the best fits to the data.

### A. S-Wave $\sigma$ Production

With the use of Eqs. (22), (23), (24), and (29), we have obtained a good fit to the data discussed in Sec. IV. The Hankel function used in Eq. (29) was of course $h_1^{(1)}$, to correspond to the $p$ wave in the elastic channel.

In Figs. 2(a), 2(b) are plotted the $\delta$ and $\eta$, respectively given by the following parameters (given also

[30] G. F. Chew, Phys. Rev. Letters **9**, 233 (1962). The static model presented in this reference gives an estimate of $\pi N$ force due to $N^*$ exchange.

[31] J. Hamilton, P. Menotti, G. C. Oades, and L. L. J. Vick, Phys. Rev. **128**, 1881 (1962), Table III.

[32] V. Singh, Phys. Rev. **129**, 1889 (1963), Appendix.

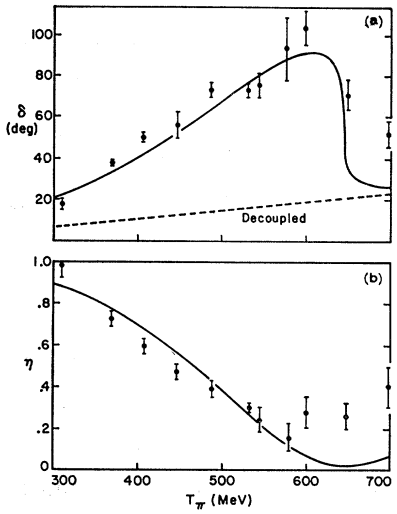


FIG. 2(a). Solid line: elastic phase shift corresponding to $\sigma$ production process with parameters given in Table I; experimental phase shifts are those from Ref. 7. Dashed line: elastic phase shift resulting from decoupling $\sigma$ channel, with other parameters as for solid line. (b) Absorption parameter corresponding to solid line in (a).

in Table I):

$$r_0=0.30\mu^{-1}, \quad f_1=0.28,$$
$$f_2=0.50, \quad f_c^2=0.74,$$
$$m^*=550 \text{ MeV}, \quad \Gamma=100 \text{ MeV}.$$

The following points may be of interest:

(a) The average mass of the $\sigma$ mass (550 MeV) is quite close to that expected from the heuristic arguments presented in Sec. II. The width of the distribution is somewhat smaller.

(b) The purely elastic scattering produced by letting $f_c^2 \to 0$ is shown as the dashed curve in Fig. 2(a). The value of the phase shift attained at 600 MeV, 20°, is not as large as that attained by Coulter and Shaw[12] without inelasticity, but is sizeable. Notice that the parametrization employed here could never reproduce the well-known crossover in the $P_{11}$ phase shift at 175 MeV. *This point is very instructive.* When an attempt was made (in the present model) to choose parameters which would yield a negative purely elastic phase shift, *it was impossible to bring it positive in a reasonable way through the inelastic mechanism.* This supports the idea that the forces are basically attractive, with some rapidly diminishing repulsive term in the amplitude. This term has been attributed to the direct nucleon pole inserted without the bootstrap conditions.[12,31]

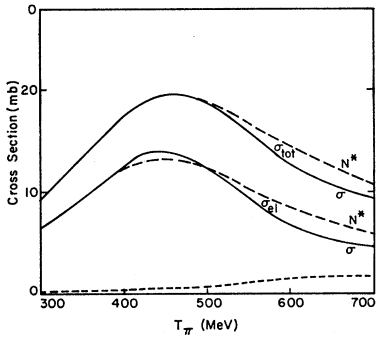


FIG. 3. Heavy curves: total and elastic cross sections from $\delta$ and $\eta$ of Fig. 2 ($\sigma$ production). Light curves: total and elastic cross sections from $\delta$ and $\eta$ of Fig. 6 ($N^*$ production). Dashed curve: result of retaining coupling leading to Fig. 2, but setting the elastic diagonal force=0.

(c) In a previous paper[25], we have shown that the $s$-wave scattering length is related to the logarithmic derivative $f$, and $r_0$ (for elastic scattering) through

$$a_0=r_0(1-f)/f. \tag{30}$$

Thus we may estimate the strength of the $\sigma N$ force in some average way. Taking $f=f_2=0.50$ and $r_0=0.30$, Eq. (30) becomes

$$a_0=0.30\,\mu^{-1}. \tag{31}$$

For comparison, this is a little stronger than the $S_{11}\pi N$ scattering length. However, the results we have obtained are rather insensitive to $f_2$ over a region around $f_2=0.50$. In particular, a value of $f_2=0.70$ gave a reasonable fit with minor adjustments in $f_c^2$. This corresponds to a $\sigma N$ scattering length of $0.13\,\mu^{-1}$ [from Eq. (30)]. Thus it is clear that one does not require a strong $\sigma N$ force, or a bound $\sigma N$ state.

(d) Because of the strength of the elastic force, the coupling (parametrized by $f_c^2$) is small. To show this, we have plotted as the lowest curve in Fig. 3 the *total* cross section obtained by using the parameters of Fig. 2, but letting $f_1=2$. This value of $f_1$ [as will be seen from Eq. (32)] produces a zero *diagonal* scattering length, and due to the $p$-wave nature of the elastic channel, virtually zero diagonal elastic forces. Thus the dashed curve plotted in Fig. 3 shows the effect of the coupling alone. The cross section shown is almost 100% inelastic, and is about 20% of the inelastic scattering obtained with $f_1=0.28$. *Thus it is largely the strong elastic force which is pulling even the inelasticity through unitarity.*

(e) The elastic and total cross sections for the best fit parameters have been plotted in Fig. 3 (solid curves). Note that the bump in the cross section is quite a bit below the position of maximum phase shift, which is a well-known property of very broad resonances. The general natures of the curves, such as position and

TABLE I. Parameters for the various curves.

| Fig. No. | Inelastic channel | $f_1$ | $f_2$ | $f_c^2$ | $m^*$ (MeV) | $\Gamma$ (MeV) |
|---|---|---|---|---|---|---|
| 2 (solid) | $N\sigma$ | 0.28 | 0.50 | 0.74 | 550 | 100 |
| 2 (dashed) | Decoupled | 0.28 | ··· | 0 | ··· | ··· |
| 3 (heavy) | Same as Fig. 2 (solid) | | | | | |
| 3 (light) | Same as Fig. 5 or 6 (solid) | | | | | |
| 3 (dashed) | $N\sigma$ | 2.00 | 0.50 | 0.74 | 550 | 100 |
| 4 (solid) | $N\sigma$ | 0.31 | 0.50 | 0.78 | 550 | 100 |
| 4 (dashed) | $N\sigma$ | 0.28 | 0.50 | 0.74 | 550 | 0 |
| 5 (solid) | $N^*\pi$ | 1.40 | 0 | 1.80 | 1238 | 100 |
| 5 (dashed) | Decoupled | 1.40 | ··· | 0 | ··· | ··· |
| 6 | $N^*\pi$ | 3.10 | 1.00 | 7.00 | 1238 | 100 |
| 7(a) | Same as Fig. 4 (dashed) | | | | | |
| 7(b) | Same as Fig. 11 (either curve) | | | | | |
| 9(a) | Same as Fig. 4 (dashed) | | | | | |
| 9(b) (curve A) | Same as Fig. 11 (curve A) | | | | | |
| 9(b) (curve B) | Same as Fig. 11 (curve B) | | | | | |
| 11 (curve A) | $N\sigma$ | 0.28 | 0.50 | 0.54 | 550 | 0 |
| (curve B) | $N\sigma$ | 0.28 | 0.50 | 0.53 | 550 | 0 |

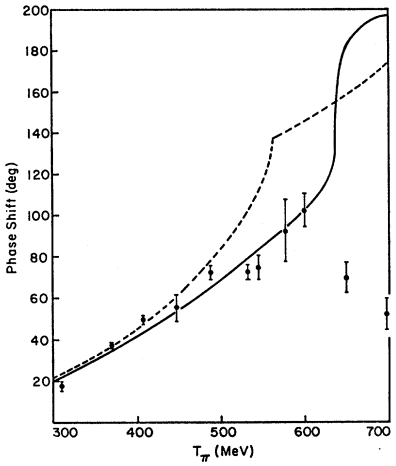


FIG. 4. (a) Solid line: result of slight changes in parameters of Fig. 2 [see Part (f) of Sec. V]; (b) broken line: result of allowing the $\sigma$ width go to 0, with other parameters as in Fig. 2.

width, are in good agreement with the results of Bareyre *et al.*,[1] which were discussed in the Introduction.

(f) The solid curve in Fig. 4 shows the phase-shift curve obtained by a slight change in the parameters describing Fig. 2. The changes were

$$\text{in } f_1\text{: } 0.28 \text{ (Fig. 2)} \rightarrow 0.31 \text{ (Fig. 4)},$$

$$\text{in } f_c^2\text{: } 0.74 \text{ (Fig. 2)} - 0.78 \text{ (Fig. 4)}.$$

All other parameters remained the same. The phase shift now goes rapidly through 90° and on past 180°. This behavior is compatible with the Bareyre[8] analysis. Of interest is the instability of qualitative behavior of the phase shift, apparent in the contrast between Figs. 2(a) and 4. We shall explore this observation in detail in Sec. VI. The absorption parameter $\eta$ has not been plotted because it looks essentially the same as the one plotted in Fig. 2(b).

(g) The dashed curve in Fig. 4 is the result of keeping all parameters the same as in Fig. 2(a), except for letting the $\sigma$ mass-distribution width go to zero. The cusp at threshold is now clearly visible. In Fig. 5(a) is plotted the absorption parameter corresponding to this dashed curve.

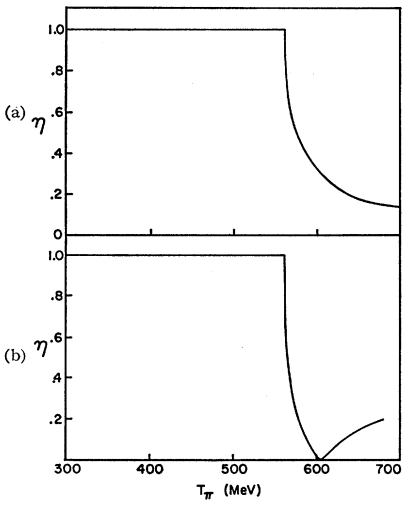


FIG. 5(a). Absorption parameter $\eta$ corresponding to Fig. 4(b). (b) Absorption parameter $\eta$ corresponding to Fig. 11 (A and B).

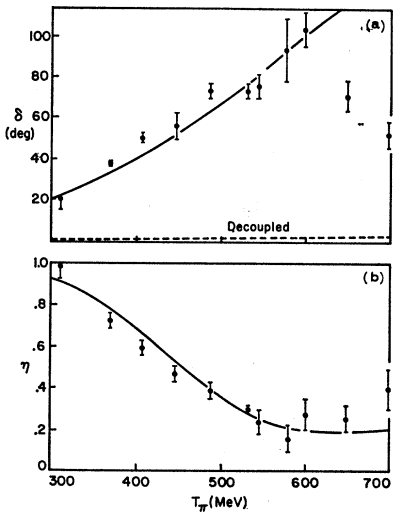


FIG. 6. (a). Solid line: elastic phase shift corresponding to $N^*$ production process with parameters given in text (Sec. V) and in Table I; experimental phase shifts are those from Ref. 7. Dashed line: elastic phase shift resulting from decoupling $N^*$ channel, with other parameters as for solid line. (b) Absorption parameter corresponding to solid line in (a).

### B. *P*-Wave $N_{33}$* Production

It turned out to be impossible to obtain a fit in which $\delta$ would turn down soon after reaching 90°. This is due to the slowness of variation of the $f_{\text{eff}}$ in the $p$-wave production case [see Eqs. (22) and (25)]. Two reasonable fits to the lower energy phases are given in Figs. 6 and 7. These have the following parameters:

| | Fig. 6 | Fig. 7 |
|---|---|---|
| $r_0$ | $0.30\mu^{-1}$ | $0.30\mu^{-1}$ |
| $f_1$ | 1.40 | 3.10 |
| $f_2$ | 0.0 | 1.00 |
| $f_c^2$ | 1.80 | 7.00 |
| $m^*$ | 1238 MeV | 1238 MeV |
| $\Gamma$ | 100 MeV | 100 MeV |

An examination of the elastic force (given by $f_1$) and the coupling $f_c^2$ gives rise to further dissatisfaction with these fits. In both cases, the values of $f_1$ and $f_2$ imply *much* less attraction in the $\pi N$ channel than in the $\pi N^*$ channel. This we can see as follows: From the properties

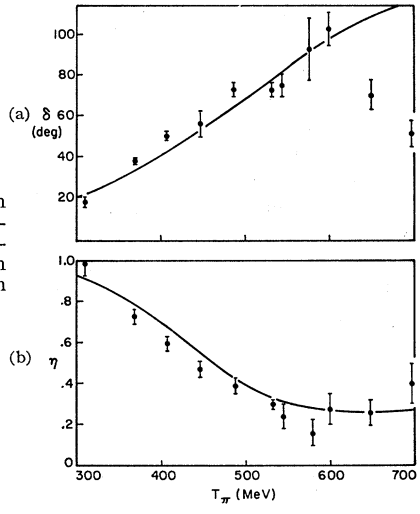


FIG. 7. See caption for Fig. 6. The different set of parameters used is given in Sec. V and in Table I.

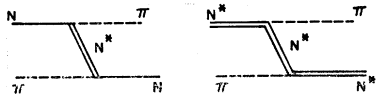


FIG. 8. Diagrams used to calculate ratio of $\pi N^*$ to $\pi N$ force.

of the little Bessel functions, we find that the $p$-wave scattering length is given in terms of the value of $f$ (the logarithmic derivative) at threshold by

$$a_1=r_0(2-f)/(1+f). \tag{32}$$

[Compare with Eq. (30) and Eq. (4.27) of Ref. 20.] Thus, the parameters of Fig. 6 imply a diagonal $\pi N^*$ scattering length of 0.67 $r_0^3$ compared to 0.02 $r_0^3$ for the $\pi N$ scattering length. These scattering lengths are to be interpreted as a gauge of the diagonal forces, much the same as with usual Born estimates. The actual $\pi N$ elastic scattering obtained by letting $f_c^2=0$ with $f_1=1.40$ (as in Fig. 6) is shown by the dashed curve in Fig. 6(a) [See dashed line, Fig. 2(a)]. The parameters of Fig. 7 yield a strongly repulsive $\pi N$ force, compared to a moderately attractive $\pi N^*$ force. Although we do not really know any of these forces, we may attempt to calculate the relative contributions from the $N^*$ exchange diagrams (Fig. 8). We pick these diagrams since they give high attraction in the $P_{11}$ state of both the $\pi N$ and $\pi N^*$ channels. In a static model by the use of the standard recoupling techniques[17] one finds that the ratio of $\pi N^*$ to $\pi N$ force in the $P_{11}$ state due to this diagram is

$$(81/64)\gamma^2{}_{N^*N\pi}{}^*/\gamma^2{}_{N^*N\pi}, \tag{33}$$

where the $\gamma$'s are the appropriate reduced widths. If we suppose that these are of the same order of magnitude, then one expects a strong $\pi N^*$ force, but not the great disparity from the $\pi N$ force which we need in order to fit.

Thus, we recapitulate our arguments against the $\pi N^*$ inelastic channel. (1) The $p$-wave nature of the final state does not allow the phase shift to drop quickly after reaching a maximum. This behavior contradicts several of the phase-shift analyses.[6,7] The cross sections, plotted as the dashed lines in Fig. 3, are reasonable fits to the Bareyre data. This illustrates the value of the phase-shift analyses in deciding on a possible mechanism for the inelasticity. (2) The strong interchannel coupling needed to create the necessary inelasticity forces us to retain a very weak elastic force, in order to keep down the lower energy phases. This is in contradiction to pole estimates of these forces.

Finally, we might say that for a correct treatment of this "resonance," one should probably couple the three channels. Coupling in the $\pi N^*$ channel would have the desirable effect of keeping up the high-energy end of the elastic phase shift in Fig. 2(a).

### C. The $\sigma$ Mass

A good fit to the data was found using a $\pi\pi$ mass distribution peaked at 550 MeV. This is in direct agreement with the requirements of some authors,[33,34] and interpolates the results of others who support enhancements around 400 MeV[35,36] and around 700 MeV.[37–39] Bryan and Scott,[33] in a consideration of $NN$ scattering, have found that, in addition to other one-boson exchange forces, the introduction of a potential due to a $0^{++}$ meson of mass 560 MeV provides a good fit to standard phenomenological potentials and to the phase shifts. Ball, Scotti, and Wong,[34] in a dispersion approach to $NN$ scattering, find that they require a mass of 540 MeV for this intermediate range attraction. We thus are in good agreement with these authors.

## VI. EIGENSCATTERING

In this section we shall explore the eigenscattering pertaining to our model. This is of twofold interest: (1) The behavior of the eigenphase shifts and mixing parameter is perhaps a truer indication of the dynamics of the problem, and (2) some of the strange variation in the recent phase-shift analyses may perhaps be explained by slight variations in these eigenparameters. We have already seen some evidence of these variations in Figs. 2 and 4. The section will consist of several parts, not all of which pertain to the central dynamical problem at hand (namely, the $P_{11}$ phenomenon), but which are of dynamical interest. First, we derive the equations giving the eigenscattering parameters from the $f$ matrix. We shall treat only the two-channel $\sigma$ production case, i.e., take our $\sigma$ pairs having a delta-function mass distribution. Secondly, we shall display some of the eigenphases of interest to the $P_{11}$ problem. Thirdly, we shall show that a type of large variation in the elastic phase shift [see in Fig. 4(a) as compared to Fig. 2(a)] caused by a small change in the $f$ matrix can be traced to a certain subtle but physically inconsequential behavior of the eigenparameters.

### A. Eigenstates of the $S$ Matrix Derived from the $f$ Matrix

Again, we treat specifically the case of $s$-wave production of $\sigma$'s with well-defined mass. We consider Eq. (1), with

$$\begin{aligned} u_1&=xA_1[j_1(x)-(\tan\delta)n_1(x)],\\ u_2&=yA_2[j_0(y)-(\tan\delta)n_0(y)], \end{aligned} \tag{34}$$

where $x=k_1r$; $y=k_2r$; $j_1$, $j_0$ are the spherical Bessel functions for $p$ and $s$ waves, respectively; $n_1$, $n_0$ are the spherical Neumann functions for $p$ and $s$ waves, respectively; and $\delta$ is an eigenphase shift.

[33] R. A. Bryan and B. L. Scott, Phys. Rev. **135**, B440 (1964).
[34] J. S. Ball, A. Scotti, and D. Y. Wong, Phys. Rev. **142**, 1000 (1966).
[35] L. M. Brown and P. Singer, Phys. Rev. **133**, B812 (1964).
[36] N. P. Samios *et al.*, Phys. Rev. Letters **9**, 139 (1962).
[37] M. M. Islam and R. Pinon, Phys. Rev. Letters **12**, 310 (1964).
[38] L. Durand and Y. T. Chiu, Phys. Rev. Letters **14**, 329 (1965).
[39] M. Feldman *et al.*, Phys. Rev. Letters **14**, 869 (1965).

The wave functions written above embody the definition of eigenscattering.[40] The normalization coefficients will be discussed presently. It is easily seen that the result of inserting (34) into (1) and demanding a nonzero solution for $A_1, A_2$ is a determinantal equation for $\tan\delta$ of the form

$$a(\tan\delta)^2+b(\tan\delta)+c=0, \tag{35}$$

where $a$, $b$, and $c$ are functions of $x$, $y$, $j_1$, $j_0$, $n_1$, $n_0$, the derivatives of the last four, and of the elements of the $f$ matrix. It is then apparent that there are two solutions, corresponding to the two eigenphases. Let us call these $\delta_a$ and $\delta_b$. From Eqs. (34), and the basic Eq. (1), we obtain for the ratio

$$\frac{A_2}{A_1}=\frac{[xj_1'(x)-f_1j_1(x)]-(\tan\delta)[xn_1'(x)-f_1n_1(x)]}{f_c[j_0(y)-(\tan\delta)n_0(y)]}, \tag{36}$$

where for typographical ease *we have taken the liberty of denoting by $j(x)$ the product of the usual spherical Bessel function with $x$, etc.*

From this equation we should like to derive the mixing parameters $\epsilon_a$ and $\epsilon_b$ describing the eigenstates of the $S$ matrix which are scattered with eigenphases $\delta_a$ and $\delta_b$. These are defined by

$$\psi_a=\cos\epsilon_a\psi_1+\sin\epsilon_a\psi_2,$$
$$\psi_b=\cos\epsilon_b b_1+\sin\epsilon_b\psi_2. \tag{37}$$

If the states are properly orthonormal, and the $S$ matrix is unitary, we should have the relation[41]

$$\tan\epsilon_a\tan\epsilon_b=-1. \tag{38}$$

What is then the proper normalization for our states $u_1$ and $u_2$ above? From a consideration of the Lippmann-Schwinger equation

$$\psi^{(+)}=e^{ik\cdot r}+\frac{1}{E-H_0+i\epsilon}V\psi^{(+)}$$

reduced to partial waves, one can show[42] that the asymptotic form of the outgoing partial wave in a channel $c'$ is

$$u_c^{(\text{out})}\sim\text{const (independent of energy)}\times\frac{1}{(v_{c'})^{1/2}}S_{cc'}\times\frac{e^{ik_{c'}r}}{r}$$

for a reaction initiated in channel $c$. Here $v_c'$ is the relative velocity in channel $c'$ and $S_{cc'}$ is an element of the unitary $S$-matrix.[43] For eigenscattering, it is then easy to see that the ratio $A_2/A_1$ is, according to our definitions of the wave functions, given by

$$A_2/A_1=(v_1/v_2)^{1/2}\tan\epsilon_a. \tag{39}$$

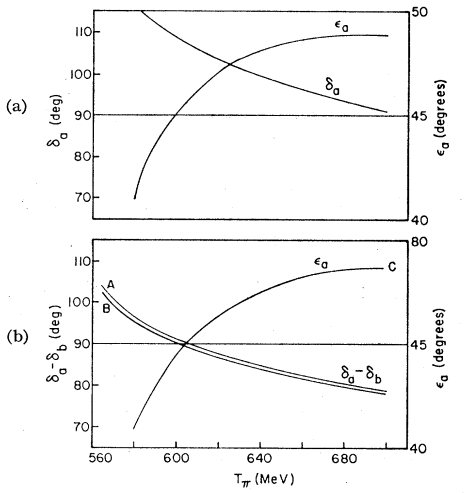


FIG. 9(a). Dominant eigenphase and corresponding mixing angle for parameters of Fig. 4(b). (b) Curve A: $\delta_a-\delta_b$ for parameters of Fig. 11, curve A. Curve B: $\delta_a-\delta_b$ for parameters of Fig. 11, curve B. Curve C: mixing angle for both cases.

Thus, armed with our expressions (35), (36), and (39), we calculate the eigenphases corresponding to Fig. 4(b). We have plotted one of these, $\delta_a$, in Fig. 9(a), along with the mixing angle $\epsilon_a$ which goes with the phase. The other eigenphase $\delta_b$ which is not plotted varies from 0° to −1° in the energy interval 565 to 700 MeV. It is obvious that while $\delta_a$ is near 90° in the interval considered, it is quite slowly varying as it comes down through 90° (in accordance with Wigner's causality condition), and cannot pull a narrow resonance. Near 600 MeV, the mixing angle goes up through 45°, making the scattering become slightly more inelastic than elastic, as far as the $\pi N$ channel is concerned. It may be added that in all calculations the relation (38) was satisfied, thus verifying our normalization of the wave functions.

We now give the reason for the behavior of the elastic phase shift in Fig. 4(b), namely, the rise toward 180°: The mixing angle goes through 45° before the difference $(\delta_a-\delta_b)$ goes down through 90°. This has been demonstrated in a recent publication[10] but we repeat the argument here for completeness. The unitary symmetric $S$ matrix may be diagonalized by the real orthogonal mixing matrix as follows:

$$\begin{pmatrix}S_{11} & S_{12}\\ S_{12} & S_{22}\end{pmatrix}=\begin{pmatrix}\cos\epsilon & \sin\epsilon\\ -\sin\epsilon & \cos\epsilon\end{pmatrix}\times\begin{pmatrix}e^{2i\delta_a} & 0\\ 0 & e^{2i\delta_b}\end{pmatrix}\begin{pmatrix}\cos\epsilon & -\sin\epsilon\\ \sin\epsilon & \cos\epsilon\end{pmatrix}. \tag{40}$$

[40] H. Feshbach and E. L. Lomon, Phys. Rev. **102**, 891 (1956).
[41] J. M. Blatt and L. C. Biedenharn, Phys. Rev. **86**, 399 (1952)
[42] M. L. Goldberger and K. M. Watson, *Collision Theory* (John Wiley & Sons, Inc., New York, 1964), p. 377.
[43] See also Ref. 29, p. 522, for an intuitive argument supporting this normalization.

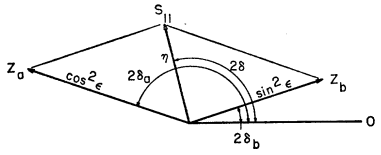


FIG. 10. Argand plot showing relation between eigenphasors and $\eta e^{2i\delta}$ [see Eq. (41) of text].

Letting $S_{11}=\eta e^{2i\delta}$, we obtain the parametrization

$$\eta e^{2i\delta}=(\cos^2\epsilon)e^{2i\delta_a}+(\sin^2\epsilon)e^{2i\delta_b}\equiv z_a+z_b. \quad (41)$$

This leads to the graphical representation of Fig. 10. Suppose we now start with some value of $\delta_a>90°$, so that $z_a$ lies in the third quadrant of the Argand plot. Suppose also that $\delta_b$ is small so that $z_b$ lies close to the ray arg$z=0$. Now let $\delta_a$ come down through 90°, while $\delta_b$ does something nondescript about 0. The resultant $S_{11}$ will lie in the third or fourth quadrant, i.e., the phase shift $\delta$ will be greater than 90°. Now let $\epsilon$ go up through 45° *before* the phases $2\delta_a$, $2\delta_b$ are 180° apart. Then as the phasors $z_a$ and $z_b$ get to anti-alignment, $z_b$ will be longer than $z_a$, and the resultant phase $2\delta$ will fly over to $2\delta_b$ through the third and fourth quadrants. That is, the phase shift $\delta$ will go from near 90° to 180° and perhaps beyond. On the other hand, if $\epsilon$ goes up through 45° *after* $\delta_a-\delta_b$ goes through 90°, then the resultant phase $2\delta$ will swing over to $2\delta_b$, with $\delta$ going *down* through 90°.

Thus, we can see that the behavior of $\delta$ in Fig. 4 is due to a combined eigenphase-shift-mixing angle behavior of the first type described above. This is explicitly shown in the curves of Fig. 9(a). To make the issue more dramatic, we have decreased the coupling $f_c^2$ until there is a transition of behavior (Fig. 11) in $\delta$, the elastic phase shift, of the type described above. In this case, $\delta_a$ still is near 90° and $\delta_b$ near 0°. We have plotted in Fig. 9(b) the difference $\delta_a-\delta_b$ for the values $f_c^2=0.54$ and 0.53, which are on either side of the transition point. On the same graph is plotted $\epsilon$. Careful scrutiny shows that $\epsilon$ goes through 45° on different sides of the transition $\delta_a-\delta_b=90°$. The near coincidence of the point where $\delta_a-\delta_b=90°$ and $\epsilon=45°$ leads to a value of $\eta$ which is virtually zero. This is seen in Fig. 5(b), where $\eta$ for both these cases is plotted. There is only one curve, since the values of $\eta$ for the two cases are practically indistinguishable. (See Table I for a listing of the parameters for these curves.)

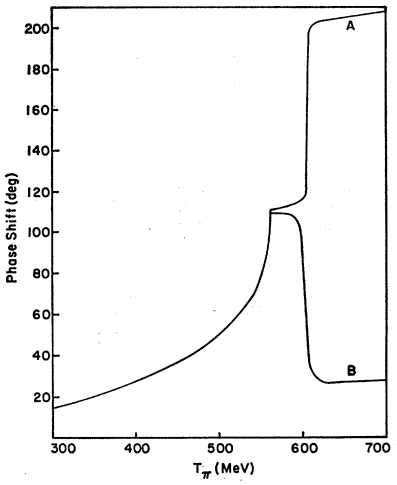


FIG. 11. Elastic phase shift at transition point discussed in text. For parameters see Table I.

It is obviously out of the question to find eigenphases for the coupling to a continuum distribution of $\sigma$'s. However, if out of the continuum of eigenchannels only a small subset has reasonable activity, then the results of the above analysis should not change markedly. Support for the last statement is provided in a comparison of Figs. 4(a) and 2(a), which shows the discussed transition occurring in the many-channel case.

## VII. THE $P_{11}$ STATE AND THE OCTET MASS FORMULA

It is valid to ask: Can the Gell-Mann–Okubo baryon octet mass formula support the existence of a "resonance" with the same quantum numbers as the nucleon? The mass formula predicts the nucleon mass to be given by

$$M_N=\tfrac{3}{2}M_\Lambda+\tfrac{1}{2}M_\Sigma-M_\Xi. \quad (42)$$

If the average masses[44] of the isotopic multiplets are inserted into Eq. (42), we obtain

$$M_N=952.2\ \text{MeV}. \quad (43)$$

The physical nucleon mass is 13.3 MeV lower. We now investigate the parameters needed to cause this depression through mixing with the $P_{11}$ object.

Let us denote by $|N\rangle$, the physical nucleon state; $|N_0\rangle$, the unmixed nucleon state; $|N'\rangle$, the physical $P_{11}$ object; $|N_0'\rangle$, the unmixed $P_{11}$ object.

We shall also let the letters themselves denote masses. If we set

$$\begin{aligned}|N\rangle&=\cos\theta|N_0\rangle+\sin\theta|N_0'\rangle,\\ |N'\rangle&=-\sin\theta|N_0\rangle+\cos\theta|N_0'\rangle,\end{aligned} \quad (44)$$

and the mass matrix

$$M=\begin{pmatrix}N_0 & \lambda\\ \lambda & N_0'\end{pmatrix}, \quad (45)$$

then by demanding a diagonalization of $M$, we obtain the relations

$$\begin{aligned}(N_0-N)(N_0'-N)&=\lambda^2,\\ (N_0-N')(N_0'-N')&=\lambda^2.\end{aligned} \quad (46)$$

Let us now assume that $N_0$ is equal to the value needed to satisfy exactly the Gell-Mann–Okubo mass formula.

[44] A. H. Rosenfeld *et al.*, University of California Report No. UCRL-8030, Part I, 1965 (unpublished).

From Eq. (43)

$$N_0=952.2\text{ MeV}. \tag{47}$$

Because of its large width, the mass of the $P_{11}$ object is difficult to specify exactly, except to say that it lies between the energy of the bump in the cross section (1400 MeV c.m.) and the energy at which the real part of the inverse partial-wave amplitude vanishes (about 1500 MeV c.m.). We compromise by taking

$$N'=1450\text{ MeV}. \tag{48}$$

Using (47) and (48) we can now solve (46) for $\lambda$ and $N_0'$, obtaining

$$\lambda=81.4\text{ MeV}, \tag{49}$$

$$N_0'=N'-13.3\text{ MeV}. \tag{50}$$

The mixing angle is given by

$$\tan\theta=(N_0-N)/\lambda, \tag{51}$$

which yields

$$\theta=9.3°. \tag{52}$$

Thus, in this picture, the physical nucleon has a 2.7% admixture of $a$, the nonoctet $P_{11}$.

We may comment briefly on the magnitude of the mixing parameter $\lambda$. It is well known that the $\Sigma\Lambda$ mass difference is quite a bit smaller than the other mass differences. We may postulate that this is due to the major part of the *baryon* mass breaking operator acting like the $F_8$ generator of $SU_3$, thus connecting only members of the same multiplet, and, in addition, not splitting the $\Sigma\Lambda$ masses. The residual mass breaking term is then a tensor $T_8^{(8)}$ (corresponding to the $D$ part), which will connect different multiplets *and* give a $\Sigma-\Lambda$ mass difference. Matrix elements of this tensor will then be of order $M_\Sigma-M_\Lambda=75$ MeV. If the $P_{11}$ is some mixture of $SU_3$ representations, this tensor will then connect it with the octet nucleon, and lead to a mixing mass of order 75 MeV. This compares well with the value we have obtained for $\lambda$ [Eq. (49)].

As for the role of the $P_{11}$ object in the $SU_3$ scheme itself, we refer the reader to a paper by Lovelace,[45] where the proposed multiplet containing the $P_{11}$ is a $\bar{1}0$, but so far there is no indication of the other members thereof, except possibly for the $I=0$, $Y=2$ member.[46] Brehm and Kane[47] have recently reported on some dynamical calculations to support this view.

## VIII. DISCUSSION AND CONCLUSIONS

We have presented a unitary inelastic model, the $f$ matrix or boundary-condition model, within whose framework we have discussed the recently reported enhancements in $I=\frac{1}{2}$ $\pi N$ scattering at a c.m. energy of 1400–1480 MeV. We have attempted to fit the Auvil *et al.*[7] $P_{11}$ phase shift and inelasticity parameter by introducing two types of inelastic channels: $s$-wave production of $I=0$, $J^P=0^+$ ($\sigma$) dipion pairs having a wide mass distribution, and the $p$-wave production of the 33 resonance. A good fit was obtained with the $\sigma$ pairs having a mass distribution centered on 550 MeV, with a width of 100 MeV. This fit also necessitated an attractive elastic force in the region of interest, an interaction radius of $0.30\,\mu^{-1}$, moderate coupling, and a moderate attraction in the $N\sigma$ channel. It was also shown that an upturning of the phase shift to go through 90° is easily obtainable by a slight change in parametrization. This was seen to result from a technicality in the dependence of the elastic phase shift on the eigenphase (Sec. VI). The fits obtained with the $N^*\pi$ production channel, although allowing a resonance, suffered from various defects. One of these was the impossibility, due to the long tail of $p$-wave production, of getting the phase shift to turn down after reaching near 90°. The latter behavior is indicated in Refs. 6 and 7. Other defects are the requirement of much more attraction in the diagonal $\pi N^*$ channel compared to the $\pi N$ channel, and the need for very strong interchannel coupling, both of which are not supported by our crude estimates of the forces.

We have presented a calculation of eigenphases within the stable $\sigma$ limit of the model, and have concluded that the eigenphase responsible for the $P_{11}$ scattering does not resonate in the region of interest. However, it does stay near 90° much of the time. The mixing angle is compatible with the experimental elastic width of the bump and stays near 45°. Finally, we have speculated that the $P_{11}$ object may be a cause of at least some of the discrepancy in the Gell-Mann–Okubo mass formula.

[45] C. Lovelace, CERN Report 65/1674/5-TH 628 (unpublished).

[46] R. L. Cool, G. Giacomelli, T. F. Kycia, B. A. Leontic, K. K. Li, A. Lundby, and J. Teiger, Phys. Rev. Letters **17**, 102 (1966).

[47] J. J. Brehm and G. L. Kane, Phys. Rev. Letters **17**, 764 (1966).